Finely-Divided Powders by Carrier Solution Injection into a Near or Supercritical Fluid

William J. Schmitt, Michael C. Salada, Gary G. Shook, and Stanley M. Speaker III
Fine Chemical Process R&D, The Upjohn Co., Kalamazoo, MI 49001

Carbon dioxide or ethane was used as an antisolvent medium from which organic solids dissolved in a liquid carrier solvent are precipitated and collected as finely divided solids. Solid compounds of pharmaceutical interest, which are virtually insoluble in the supercritical fluids per se, are efficiently obtained by injecting a solution of the solid into a volume of stirred supercritical fluid or compressed liquefied gas. A free-flowing powder comprising very small particles (< 5 μm) is obtained. Both continuous-flow and batch operations were developed although the continuous-flow operation is preferred. Process variables including temperature, pressure, stirring rate, injection concentration, and the rate and temperature of the carrier solution injection were studied to see how they affect the physical properties of the resultant product. Recovery (yield), particle size and uniformity, bulk powder density, microscopic appearance, and surface area were measured. Carbon dioxide and ethane antisolvents, several liquid-phase injection solvents, and different solid compounds were studied. A simple unsteady-state mathematical model of this CSTR precipitator is also presented.

Introduction

The practice of dissolving a solid substance in a minimum amount of a good liquid solvent and then adding it to a large amount of a poor solvent to effect almost immediate precipitation of the dissolved solid is well known in the chemical industry (McCabe and Smith, 1976). Likewise, the reverse process, where the poor solvent is added to the solute dissolved in the good solvent, is also well known (Kirk-Othmer, 1979). The first method is sometimes referred to as a controlled "micro-precipitation (or microcrystallization)," and the second as a product "knock-out" or "salting-out." Both methods take advantage of the fact that a solid phase will re-form if the solvent environment around the dissolved solute is changed from subsaturation to supersaturation. In a simple crystallization this is done by increasing the concentration of the solute or by reducing the temperature of the solution, or both. In the preceding examples the composition of the solution is changed dramatically by the addition of a third component, the liquid antisolvent.

Both methods tend to produce small particles due to the sudden change in solubilization environment and diminishingly small intraparticle mass transfer of the solute in the antisolvent liquid. One disadvantage to these techniques is that small particles often form claylike filter cakes that filter poorly. Another consequence of liquid microprecipitation is that the resultant particle-size distribution of the isolated particles is rather broad. Some large particles are formed.

Similarly, the process of dissolving a solid substance in a supercritical fluid, and then flashing the supercritical fluid solution through a valve or an orifice to produce fine particles of the solid is also now a familiar technique (Paulaitis et al., 1983; Debenedetti and Tom, 1991; Matson et al., 1989). This technique produces very small uniform particles, often less than 3 micron diameter, but is limited on a production scale by the solubility of the solid in the supercritical fluid. Unfortunately, many compounds of pharmaceutical interest are either too polar or of too high a molecular weight to be more than sparingly soluble in commonly used supercritical fluids with near-ambient critical temperatures. The addition of an entrainer (cosolvent) to the supercritical fluid may improve the solubility of the solid, but then the isolation of the solid as dry, free-flowing powder becomes a challenge of not allowing the entrainer to condense with the solid upon pressure reduction.

Correspondence concerning this article should be addressed to W. J. Schmitt.

Our work attempts to circumvent this low solubility problem by regarding carbon dioxide or ethane as an antisolvent and inducing rapid crystallization by injecting a solute solution into an agitated volume of supercritical or near-critical antisolvent. Due to the lack of surface tension and low viscosity of a supercritical fluid, it was hoped that some of the characteristics of supercritical pressure flashed powder could still be retained in a supercritical fluid antisolvent precipitation. Another benefit is the ability of the supercritical antisolvent to filter rapidly through the accumulated fine particle cake.

Other researchers have recently reported that they are experimenting with this new way of utilizing supercritical fluids (Gallagher et al., 1989; Fischer, 1991; Yeo et al., 1993; Dixon et al., 1993). Stahl et al. (1984) described their efforts to extract the vegetable oil from viscous crude lecithin in a spray tower, leaving as product a light-colored powder comparable in consistency to commercially available purified lecithin powder. The authors, however, state that attempts to reduce the viscosity of the crude lecithin by warming or by addition of a diluent solvent gave unsatisfactory results. The work by Gallagher et al. describes dissolving an organic solid in a liquid solvent such as acetone, and then adding liquefied carbon dioxide (antisolvent) to the solution, eventually causing precipitation of small particles as the solution composition changes. This is a batch process and is in effect the reverse of the process described here. The patent by Fischer describes the preparation of spheres containing an active drug embedded throughout a second solid, such as polylactic acid, to produce a sustained release formulation of the active drug. The solids can be dissolved in a suitable liquid solvent and precipitated into supercritical carbon dioxide in a spray tower. From our point of view, rather large spheres (e.g., 100 μm) are said to be produced. The work by Yeo et al. presents a similar technique to that described in this work. Insulin was dissolved in dimethylsulfoxide and sprayed into a continuously flowing mass of either supercritical or near-critical carbon dioxide. Spherical particles of insulin with average diameters in the range 1–4 microns were produced. Quite remarkably, the insulin was not denatured during the high-pressure processing, but retained its biological activity as measured by blood glucose level in rats. We also routinely obtain particles in the range less than 10 microns, but since our model compounds are not biologics, loss of activity due to processing would not seem to be a concern. Dixon et al. present a thorough analysis of the supercritical fluid antisolvent microprecipitation process and give it the name "PCA." They present systematic data concerning the precipitation of polystyrene over a wide range of conditions, much as pharmaceutically useful medium molecular weight steroids are examined in this study.

Theory

The nucleation and growth of crystals from solution is an area combining concepts from thermodynamics, kinetics, and mass transfer. The formation of small particles (on the order of 1–5 μm) by injection of an organic carrier solvent nearly saturated with dissolved solid, into a large volume of supercritical fluid (in which the dissolved solute has very poor solubility), is simply a "salting out" crystallization, whereby the driving force for solid formation is a sudden and large change in the environment of the neutrally charged (organic) solute molecules. This article will, however, refer to the process as a "microprecipitation," as it is specifically intended to form solid particles, crystalline or amorphous, of as small a diameter as possible.

Table 1. Table of Properties for CO_2, Ethane, Pentane, and Water at 20°C

Compound	Pres. bar	Dens. g/cm^3	Visc. cP	Diff. cm^2/s	Surf. Ten. dyne/cm
Water	1.0	0.998	1.002	3.37×10^{-5}	73.0
Pentane	1.0	0.626	0.240	4.21×10^{-5}*	18.2 (25°)
CO_2	57.4	0.760	0.073	3.1×10^{-4}†	1.16
C_2H_6	37.7	0.335	0.039	3.9×10^{-4}‡	0.97§

*Hexane at 25°C (Reid et al., p. 609, 1987).
†CO_2/naphthalene at 20°C and 58 bar (Reid et al., p. 594, 1987).
‡Saturated liquid ethane at 20°C and 37.6 bar (Gaven et al., 1962).
§Estimated (Reid et al., p. 637, 1987).

There are several theoretical aspects of this supercritical microprecipitation process that will be cursorily mentioned, as each (and perhaps others) seem to play some role in the mechanism. Although each aspect has been studied in detail for behavior in liquids, the transitions to behavior in supercritical or near-critical fluids has generally not been made. The point that we primarily wish to establish is that by using a supercritical fluid antisolvent, the unique viscosity, density, diffusivity, and interfacial surface tension properties may be responsible for the small, relatively uniform diameter of the particles so produced. A comparison of the properties of some commonly used liquid and supercritical antisolvents is shown in Table 1.

The theoretical basis of our technique is relatively simple. A stream of carrier solvent containing dissolved solid compound is injected into an agitated volume of supercritical or near-critical antisolvent. Antisolvent rapidly diffuses into the thin carrier stream jet as the carrier solvent counterdiffuses into the antisolvent. Rapidly, the solute molecules nucleate and crystallize as their ability to remain dissolved vanishes. Large crystal growth is inhibited due to the lack of mass transport in the very poorly solubilizing fluid antisolvent.

One limitation to the technique is that the carrier solvent and the fluid antisolvent must be at least partially miscible. If immiscibility develops in the mixing chamber, two fluid phases will form, the solute will remain dissolved in the carrier solution rich phase, and will pass through the filtration collector (poor recovery). Even if some solid particles are formed, their integrity may be poor (large crystals or sintered particles) due to excessive solubility in the carrier solvent-rich phase. Water is the principal offender, as discussed later.

Mixing of miscible liquids

One of the potential advantages of the near or supercritical fluid precipitation is that the mixing of the injection stream into the bulk of the antisolvent can occur faster due to the

$$N_{Re} = \frac{nD_a^2\rho}{\mu} \tag{1}$$

lower viscosity and higher diffusivity of the near-critical antisolvent. To check this, one correlation for mixing time in baffled tanks with six-bladed impellers gives that the time of mixing is a function of the Reynolds number at the tip of the impellers.

With our 5.08-cm-dia. impeller operating at $n = 1{,}200$ rpm, we find that $N_{Re} = 51{,}400$ for water at 20° C, but that $N_{Re} = 537{,}300$ for liquid CO_2 at 20° C (density ρ and viscosity μ from Table 1). From a well-known standard correlation (Norwood and Metzner, 1960):

$$f_t = \frac{t_T (nD_a^2)^{2/3} g^{1/6} D_a^{1/2}}{H^{1/2} D_T^{3/2}} = \text{function } (N_{Re}), \qquad (2)$$

where f_t is a monotonically decreasing dimensionless blending-time factor derived from experimental data, t_T is the blending time, n and D_a are as in Eq. 1, g is the gravitational constant, H is the filled liquid depth (30.96 cm in our autoclave), and D_T is the tank diameter (8.41 cm). From the graph we find that $f_t = 5.8$ for water and 5.1 for carbon dioxide. The correlation is nearly horizontal for $N_{Re} > 50{,}000$. Translating this into blending time, the correlation predicts a blending time of approximately 1.7 seconds if the autoclave was filled with water and about 1.5 seconds if filled with liquid carbon dioxide, despite the order of magnitude difference in Reynolds number. This suggests that physical stirring rate may not be a strong factor in the production of fine particles in the supercritical fluid microprecipitation technique above a minimum stirring rate. Molecular diffusion may be a more significant factor influencing the antisolvent penetration of the injected solution stream. Further discussion concerning droplet formation and the mass transfer between supercritical antisolvent and liquid carrier solvent can be found in the article of Dixon et al. (1993).

Nucleation

From the theory of chemical kinetics, the rate of nucleation, B^0 is given by the equation (McCabe and Smith, 1976):

$$B^0 = C \exp\left[- \frac{16\pi\sigma^3 V_m^2 N_a}{3\nu^2 (RT)^3 (\ln \alpha)^2} \right] \qquad (3)$$

The preceding expression is often used to examine the relative importance of factors in the theory of homogeneous nucleation. In this equation σ is the surface energy of a crystal face, V_m is the molar volume, N_a is the Avogadro constant, ν is the number of dissociated ions from the solute ($\nu = 1$ for our nondissociating organic solute), R is the gas constant, and T is the absolute temperature. The other quantities are defined below.

The purpose here is not to use the equation to estimate the actual number of nuclei formed per second per unit volume (B^0), since the frequency factor C is not even roughly known for precipitation in a supercritical fluid. Rather, the purpose is to show that the value for α is extremely large for injection microprecipitation and this, being in the denominator, would indicate that a very large number of nuclei might be expected to form compared to the usual crystallization situation where the solution is only slightly supersaturated. To supplement this study, the solubility of methylprednisolone acetate in pure carbon dioxide at 26°C and 149 bar was measured in a conventional packed column experiment and was found to be $y_{MRA} = 6.7 \times 10^{-6}$ (mole fraction). The saturation solubility of methylprednisolone acetate (MRA) in tetrahydrofuran at 21°C is 0.103 g/mL or 0.0196 mol fraction. If the solute is being injected at 90% saturation, then

$$\alpha = 1 + (y_{act} - y_{sat})/y_{sat}$$
$$= 1 + [(0.0176 - 6.7 \times 10^{-6})/6.7 \times 10^{-6}] = 2{,}630. \qquad (4)$$

Although the injection of a solution into an antisolvent is far from an equilibrium technique, this analysis qualitatively indicates that a large number of nuclei may be formed compared to conventional cooling and/or solvent exchange techniques where the value of α is close to unity.

Experimental Apparatus

The main supercritical fluid apparatus is similar to several that have been described in the literature (Schmitt and Reid, 1986). A conventional 2.54 cm o.d. × 30.5 cm vertical column extractor with a water bath was used to measure the equilibrium solubility of methylprednisolone acetate in compressed carbon dioxide at 26°C as described earlier. The supercritical fluid microprecipitation equipment centers around a 2-L stirred autoclave. All liquid-bearing surfaces are type 316 stainless steel unless noted otherwise. The autoclave is supplied with high-pressure liquefied gas by means of the diaphragm gas compressor. The double-ended compressor is capable of delivering 495 cm^3/min liquid at 500-psi (3.4-MPa) inlet pressure. To ensure that the maximum possible flow of liquid carbon dioxide or ethane is delivered, the fluid is cooled to ca. 0°C immediately before supplying the compressor. The gas cylinder is equipped with a length of flexible tubing and stands on a floor scale, thus weighing the cylinder as an experiment progresses. The compressor actually charges a 1-L pressure reservoir which is maintained at a pressure about 20 bar greater than the desired run pressure by means of a pressure-sensing gauge that cycles the compressor as the pressure in the reservoir rises and falls around ±3 bar of the setpoint. The actual system pressure in the autoclave is maintained constant by means of a pressure-regulating (Tescom) valve. Pressure is read by means of a test gauge (0–400 bar) and simultaneously by an electronic pressure transducer (Helicoid) connected to the autoclave by 0.32-cm tubing. Temperatures are measured with 0.16-cm copper-constantan thermocouples positioned at various locations in the apparatus and read from a digital indicator. This design is typical of SCF extraction equipment.

A detail of the autoclave, which serves as a mixing, precipitation, and filtration chamber is shown in Figure 1. A "collection basket" (filtration chamber) was specially constructed to slide down into the cylindrical bore of the bolted-closure autoclave. The bottom of the basket is a removable 2-μm (8.4-cm-dia.) sintered metal filter plate (Fuji plate) that collects the solid product but allows the CO_2/organic solvent "filtrate" to pass through. A 10-micron plate was first tried but allowed powder through the weave. A 5-micron plate was

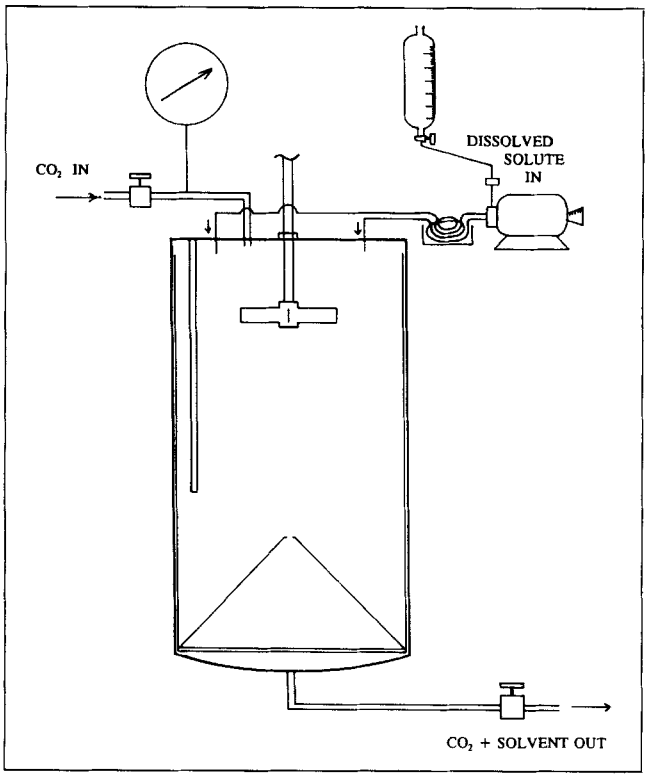

Figure 1. Continuous supercritical fluid microprecipitation chamber apparatus.

satisfactory, but the 2-micron filter plate is thought to be optimal. (The 2-micron plate may be close to restricting fluid flow during fast depressurization.) The supercritical fluid filtrate exits from the bottom of the autoclave and, after depressurization through a valve, is vented. The autoclave is equipped with a 5.08-cm six-bladed turbine agitator positioned 9 cm below the top of the autoclave so that mixing is best in the upper region. A hollow conical baffle (9.5 cm in height) is placed at the bottom of the chamber during a run to diminish the possibility of fluid short-circuiting through the chamber without adequate mixing. The baffle has a 0.32-cm hole drilled at its apex through which some of the antisolvent/particle slurry passes (some may pass around and under the cone base and some powder remains above the cone). Yields were erratic without the baffle; with the baffle yields are much more reproducible.

Pure antisolvent (CO_2 or C_2H_6) is fed to the autoclave by means of the gas compressor/reservoir previously described. The pressure regulator delivers liquid as needed to maintain the desired autoclave operating pressure. System temperature from -20°C to 90°C can be obtained by supplying either cold ethanol or steam/water to the autoclave jacket. A double-headed high-pressure metering pump (Milton-Roy, 460 mL/h) is used to inject the "injection solution" (solid dissolved in carrier solvent) into the autoclave during an experiment. Two 0.16-cm-OD by 0.051-cm-ID valved lines, one from each head, inject the solution into two top ports on the autoclave and protrude about 6 mm into the mixing chamber. No distributer or spray head is used. The lines are coiled and pass through a glass dish that can contain hot or cold water to achieve different injection temperatures if desired. The lines are thermally insulated up to their attachment point on the autoclave. The metering pump is supplied via PTFE line from a 500-mL jacketed glass addition funnel that serves as the injection solution reservoir. The injection solution passes through a 2-μm in-line filter prior to the metering pump inlet. The autoclave filtrate is vented directly into a fume hood by means of valve and tubing as shown. We found it necessary to wrap the valve with heating tape to avoid dry ice formation. With the heating tape operating, the outlet valve (a 0.64-cm regulating stem valve) maintains a fairly constant outlet flow of fluid from the system with some operator assistance. The temperature of the autoclave chamber is measured by means of a thermocouple positioned in the thermocouple well.

Example of a Supercritical Fluid Microprecipitation

Methylprednisolone acetate (15.0 g) was dissolved in 150 mL of tetrahydrofuran (THF, spectrophotometric grade, no stabilizer) to make a saturated solution at 21°C. This solution was filtered through a polishing filter and an additional 15 mL of THF was added to make a 10% subsaturated solution of the steroid suitable for injection into the autoclave. The autoclave "basket" was then prepared. The 2-micron metal filter plate was fit into the bottom of the collection chamber, the conical baffle was placed on top of the filter plate, and the baffle was secured with a press fit PTFE ring. The basket was then inserted into the autoclave and a tight-fitting PTFE sealing annulus was pressed into place on top of the basket. The purpose of this top gasket is to prevent fluid and fine particles from channeling in the narrow gap between the inner wall of the autoclave and the outer wall of the basket sleeve, thereby avoiding collection. The autoclave head was then placed on the apparatus and bolted. The autoclave was purged of air by twice filling with carbon dioxide to 5 bar and venting from the bottom. Heating of the autoclave jacket with 60°C water was begun (later cut back to 53°C to maintain a 45° system temperature). The autoclave was then pressurized with carbon dioxide to 155 bar. The 179 mL of methylprednisolone acetate/tetrahydrofuran injection solution was added to the 500-mL reservoir. Agitation was begun and set to 1,200 rpm.

The run began by establishing a steady-state flow of carbon dioxide at approximately 35 g/min while setting the regulator to maintain 151 bar. The flow of carbon dioxide was regulated by manual operation of the bottom outlet vent valve. The flow rate was controlled by observing the rate of pressure fall in the CO_2 surge tank. The actual mass-flow rate was measured by recording the changing weight of the main CO_2 supply cylinder. When steady state was established and the system temperature was 45°C, the injection was begun by switching on the metering pump and simultaneously opening the shut-off valves in the 0.16-cm injector lines. The metering pump flow rate settings were preset to deliver 1.4 mL/min per line for a total injection solution flow rate of 2.8 mL/min. Both lines are always set to inject at the same rate, but their strokes are 180° out of phase. The heating/cooling bath was not used in this experiment, so the injection was made at 22°C (room temperature).

The run proceeded routinely for the next 65 min until all of the injection solution was injected. The operator's only

continuous duty is to maintain the flow of CO_2 constant by manipulating the autoclave vent valve as necessary, and to record data every 10 min. The CO_2/THF stream was vented and is not reused. When the injection solution reservoir was empty, a 12-mL THF rinse was quickly added to displace THF/methylprednisolone acetate solution from the pump lines. The metering pump was then turned off, but an additional 2.3 kg of carbon dioxide was injected at the steady-state flow rate and pressure to purge THF from the stirred system (approximately 1.1 kg of CO_2 is needed to fill the 1,790-mL internal volume of the collection chamber). If this final purge with pure antisolvent is not done, solvent (THF) will condense at some point during the final depressurization and "rain" on the collected powder, ruining its integrity. Yield could also be lost due to resolubilization of the powder in the THF phase. Not using a sufficient quantity of purge gas for the volume of the system or the length of the run may be detrimental to the product. This purge cycle is further discussed in the mathematical modeling section. The jacket heating was discontinued.

When the 2.3 kg of pure CO_2 had been added, the antisolvent (CO_2) inlet was closed while the exit (vent) stream was left open. The autoclave was slowly depressurized over 45 min. The pressure first dropped quickly to about 55 bar, but then remained fairly constant through the region of discharging liquid. The internal temperature of the autoclave fell to 22°C due to expansion. Care must be taken to maintain a slow venting through this long isobaric regime so as to avoid violent boiling that can disrupt the bottom metal filter plate, allowing product to escape. If the temperature of the fluid being vented is above its critical temperature, the depressurization can proceed faster, as boiling will not occur unless the fluid under the filter plate cools locally to lower temperature. In either case a cautious depressurization is advisable. When the pressure equilibrated with the atmosphere, the autoclave was opened. The inner basket collection chamber was lifted out of the apparatus and was weighed after temperature equilibration in a nitrogen box.

The product was 13.50 g (90% recovery) of a very finely divided, slightly cohesive or "staticy" white powder of methylprednisolone acetate resembling powdered sugar. The powder was easily removed from the metal collection chamber simply by inverting the chamber. Some product was found above the baffle cone, but most of the product was found under the baffle on top of the 2-micron filter plate. The powder was submitted "as is" for physical analysis, but could have been dried further in a vacuum oven or in the autoclave to remove trace THF odor or to degas it completely of residual CO_2. The product contained 0.01 wt. % THF residual solvent, and had a geometric volume-mean (GVM) particle size of 6.3 μm, a surface area of 1.9 m^2/g, and was the usual (desired) crystal form of methylprednisolone acetate by XRD analysis. Residual solvent was determined by gas chromatography using a 60-m DB-5 capillary column. Particle size was measured in one of two ways, either with a Coulter Counter apparatus (Elzone 280PC, Particle Data Corp.), in which the powder was suspended in aqueous electrolyte and passed through a 30-micron orifice, or simply by examining a sample of the powder with a light microscope, utilizing a Nikon calibration slide with 10-micron (0.01-mm) divisions. In Tables 2–11 Coulter Counter results are reported as the GVM average diameter to 0.1-micron accuracy. When calibrated light microscopy is reported, a range of particle size (such as 4–8 μm) is reported indicating the observed diameters of the vast majority of particles in the sample. Specific surface area was measured with a Quantichrome Quantasorb instrument measuring nitrogen adsorption by the dynamic flow method. The surface area was then calculated utilizing the Brunauer–Emmett–Teller (BET) model. Powder bulk specific volume (or reciprocal bulk density) was measured by means of a standard tapping procedure. A known weight of the sample powder was placed in a 25-cm^3 glass graduated cylinder and was repeatedly tapped up to 300 times until the powder did not compact any further. Then the "tapped" specific volume of the powder in cubic centimeters per gram was calculated. In the few cases that powder X-ray diffraction (XRD) analysis was performed, it was done on a Siemens D500 diffractometer scanning from 3 to 40 deg 2θ.

Discussion of Results

The primary purpose of the antisolvent microprecipitation is to obtain small particles in high yield. The properties of the finished powder, such as its bulk density and rate of dissolution, are also of interest. Therefore, the effect of systematically changing process variables on the outcome of the microprecipitation has been examined. The model compound methylprednisolone acetate (MRA) was used throughout these experiments except for the hydrocortisone acetate also appearing in Table 5.

The effect of stirring rate

The average size of the particles formed in a "salting out" precipitation depends on how quickly the antisolvent penetrates the solute/good solvent environment. Although ultimately homogeneity must occur on a microscopic level, the rate at which the solutions are physically blended is a critical process variable. When the size, shape, and placement of the agitator remains constant, then the power of agitation delivered to the fluid is directly proportional to the speed of revolution. The effect of rpm on the CO_2/THF/MRA system is shown in Table 2.

Table 2. Effect of Stirring Rate on the CO_2/MRA/THF System

Temp. °C	Pres. bar	Dens. g/cm³	Stir. rpm	CO_2 Flow g/min	Inj. Rate mL/min	Yield wt. %	Tapped Sp. Vol. cm³/g	Part. Size μm
26	151	0.871	300	95.0	2.5	99.6	2.21	3.1
26	151	0.871	900	100.0	3.1	80.0	2.04	4.4
25	152	0.877	1,500	84.0	2.6	98.6	2.08	4.8

Table 3. Effect of Temperature at Constant Pressure for CO_2/THF/MRA

Temp. °C	Pres. bar	Dens. g/cm^3	CO_2 Flow g/min	Inj. Rate mL/min	Yield wt. %	Tapped Sp. Vol. cm^3/g	Surf. Area (BET) m^2/g	Part. Size μm
−6	151	1.025	40.0	2.7	93.0	7.9	3.5	2.5
21	151	0.898	41.0	2.7	91.3	8.2	3.2	2.7
44	151	0.749	36.0	2.7	90.0	5.0	1.9	3.0
63	151	0.574	40.0	2.7	90.7	2.0	0.8	3.2
				USP Air Jet Micronized		3.3	ca. 2–3	2.2
				Pentane Knockout (20°C)		9.0	—	3.4

Table 4. Effect of Temperature at Constant Pressure for ETHANE/THF/MRA

Temp. °C	Pres. bar	Dens. g/cm^3	C_2H_6 Flow g/min	Inj. Rate mL/min	Yield wt. %	Tapped Sp. Vol. cm^3/g	Surf. Area (BET) m^2/g	Part. Size μm
−6	100	0.444	36.0	2.9	93.7	13.2	4.2	2.6
21	100	0.394	21.9	2.9	92.7	22.5	3.3	2.6
56	100	0.295	36.0	2.9	94.3	8.9	3.1	3.0

Table 5. Effect of Temperature at Constant Pressure for CO_2/Dimethylformamide/Hydrocortisone Acetate

Temp. °C	Pres. bar	Dens. g/cm^3	CO_2 Flow g/min	Inj. Rate mL/min	Yield wt. %	Tapped Sp. Vol. cm^3/g	Part. Size μm
21	110	0.855	106	2.3	83	7.5	8.5
45	150	0.741	70	2.9	45	4.2	8.4
65	150	0.553	79	1.8	68	2.6	7.8

The best information from these experiments comes from microscopic examination of the product. For the 300-rpm conditions, there were some very large crystals of methylprednisolone acetate formed (15–30 μm) interdispersed among the generally smaller product. At 900 rpm no very large solids were seen, although some 10–15 μm rods were observed on the slide. At 1,500 rpm there were still a few 10–15 μm particles. The Coulter Counter particle size and the tapped powder density data clearly show this trend. From these experiments it was inferred that 900 rpm may be as effective at mixing as 1,500 rpm, but that stirring rate was a limiting factor below 900 rpm. Therefore all future experiments studying other processing conditions were run at 1,200 rpm.

The effect of temperature at constant pressure

Altering the temperature of the antisolvent plays an important role in determining the characteristics of the microprecipitated solid, as shown in Tables 3, 4 and 5 for a combination of different antisolvents, solutes, and injection solvents. In all cases the injection temperature was ambient (ca. 20°C).

These data show that colder antisolvent temperatures favor higher specific bulk volumes, higher surface area, and smaller particles. This effect can, in part, be linked to the difference in temperature between the injection solution and the antisolvent, as discussed below. The yields are generally higher at the colder temperatures. Also measured in this group were the bulk-powder specific volume and particle size for air-impact micronized (jet milled) MRA, and MRA dissolved in THF and added to rapidly stirred pentane at 20°C.

Figure 2 shows this marked relationship between bulk-powder density and antisolvent (system) temperature for methylprednisolone acetate and carbon dioxide. The air impact micronized solid is rather dense as a powder despite its small particle size. The pentane microprecipitated material is very fluffy, but this may be due to the fact that some large needles were produced (microscopic examination), which do not pack well in the tapping test. In Table 5 results with hydrocortisone acetate are also given. The 45°C and 65°C data are at constant pressure. The recoveries (yields) vary widely because a 10-μm filter plate and no cone baffle were used in this early experiment. The trend of "colder temperatures makes a fluffier solid" can clearly be seen in Tables 3 and 5, but the trend is not precisely followed for the ethane/MRA

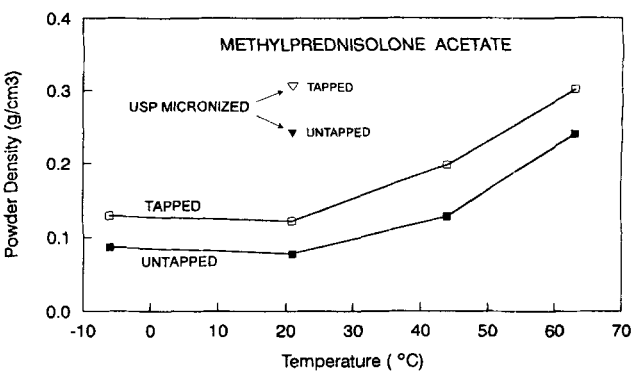

Figure 2. Microprecipitated powder density vs. temperature.

Table 6. Effect of Pressure at Constant Temperature for CO_2/15% MeOH: 85% CH_2Cl_2/MRA

Temp. °C	Pres. bar	Dens. g/cm³	CO_2 Flow g/min	Inj. Rate mL/min	Yield wt. %	Tapped Sp. Vol. cm³/g	Part. Size μm
26	102	0.810	61.0	2.23	100	4.3	2.1
23	276	0.963	42.2	2.4	98.6	4.3	2.4

system (Table 4). In all cases, however, the warmest temperatures produced the densest (least voluminous) powder and the colder temperatures the fluffiest powder, as measured after tapping.

The effect of pressure at constant temperature

The antisolvent (CO_2) pressure was varied from 100 to 280 bar at 25°C as shown in Table 6. The pressure does not seem to have much effect on the properties of the product, although at lower pressures the concentration of carrier solvent builds to a higher concentration in the chamber, and slightly more residual solvent may be found in the final product. Satisfactory product can be obtained at lower pressures, thereby minimizing the processing costs.

The effect of temperature at constant fluid density

A series of three experiments were performed in which the temperature and the pressure of the antisolvent CO_2 were varied so as to obtain the same CO_2 density, as shown in Table 7. For each, 15 grams of MRA was dissolved in 75 mL of 15% methanol/85% CH_2Cl_2 solvent and injected into flowing carbon dioxide.

The yield decreases at the highest temperature, probably due to the increased solubility of the steroid. The specific surface area results are erratic, but could be said to be essentially the same. Microscopic examination of the three products showed a significant difference; the low temperature run produced the smallest and most uniform particles of the series, the 21°C experiment gave slightly larger particles, and the 39°C run gave the largest particles and the greatest disparity between the smallest and the largest particle seen on the slide. The particle size of the 21°C product was accurately determined to be 8.2 micron GVM diameter by Coulter Counter analysis, but the 5.5°C and the 39°C samples did not run well through the instrument, so GVM particle size is not reported here.

The relationship between antisolvent temperature, density, droplet size, and other factors is also discussed in the article by Dixon et al. Similar to our findings with steroid solutes, they report that the size of the polymer particles increases significantly as the system temperature is increased. They also report that polymer morphology does not change significantly with changing CO_2 density (or pressure) if the antisolvent temperature remains constant, as we observe for various pressures under isothermal conditions (Tables 3, 4 and 5). Their injections were designed so that the polymer solution was injected into the antisolvent at essentially the temperature of the antisolvent itself. Thus there seems to be accumulating evidence that the antisolvent temperature, more than the pressure or density, influences the size and morphology of the solid product obtained.

Since the antisolvent pressure has negligible effect on the particle size, it could be suggested that the antisolvent temperature is more responsible for the size differences. However, even this might not be the complete explanation. In one case ambient temperature injection solution was injected into cold antisolvent, and in another case ambient solution was injected into warm antisolvent.

Effect of ΔT between injection solution and antisolvent

Another factor expected to influence the size and other characteristics of the particles formed is the difference in temperature between the injection solution and the antisolvent. Results for two series of experiments are given in Table 8 for carbon dioxide and in Table 9 for ethane.

For the carbon dioxide, the trend is very clear that adding hot injection solution into cold antisolvent produced small uniform particles, and the greater the temperature difference, the smaller the particles. This also produced tapped bulk-powder specific volumes that followed the trend of the "most voluminous powder produced from the greatest positive temperature differential," that is, hot into cold makes fluffy material, whereas cold into hot makes a denser material. For the ethane experiment the hot-into-cold experiment clearly gave the smallest and most uniform particle size, whereas same temperature injection and cold into hot produced similar looking material of larger particle size from microscopic examination. The tapping experiments did not follow the usual trend.

Table 7. Effect of Temperature at Constant Antisolvent Density for CO_2/15% MeOH:85% CH_2Cl_2/MRA

Temp. °C	Pres. bar	Dens. g/cm³	CO_2 Flow g/min	Inj. Rate mL/min	Yield wt. %	Surf. Area (BET) m²/g	Part. Size μm
5.5	51	0.902	95.0	3.7	95.7	0.9	Small ca. 4–6
21	150	0.898	60.0	2.5	97.2	1.4	8.2
39	284	0.904	83.0	2.8	91.3	0.8	Large ca. 10–15

Table 8. Effect of ΔT between Injection Solution and Antisolvent Fluid for CO_2/THF/MRA

Temp. °C	Pres. bar	Dens. g/cm^3	Inj. Temp. °C	ΔT °C	CO_2 Flow g/min	Inj. Flow mL/min	Yield wt. %	Tapped Sp. Vol. cm^3/g	Part. Size μm
25	150	0.876	80	+55	91.0	2.3	94.3	4.5	Large 18.5
−7	151	1.029	80	+87	67.0	2.2	83.7	6.4	Small 7.32
55	152	0.655	−15	−70	45.0	2.2	98.6	4.0	Wide 20.1

Table 9. Effect of ΔT between Injection Solution and Antisolvent Fluid for ETHANE/THF/MRA

Temp. °C	Pres. bar	Dens. g/cm^3	Inj. Temp. °C	ΔT °C	C_2H_6 Flow g/min	Inj. Flow mL/min	Yield wt. %	Tapped Sp. Vol. cm^3/g	Part. Size μm
25	152	0.409	23	−2	36.0	3.4	98.7	6.0	Medium 25.8
−6	155	0.457	84	+90	38.0	2.8	94.0	5.3	Small 12.4
52	155	0.361	−16	−68	45.0	3.3	98.7	6.3	Medium 15.0

These experiments indicate that injecting warm solution into a cold antisolvent is strongly influential in the production of small particles.

Effect of injection solution concentration

A moderately strong effect of particle size with various injection solution concentrations was observed in one set of experiments as shown in Table 10. The smallest particles (and also the most uniformly sized particles) were produced with 60% saturated injection solution. By light microscopy, the 90% saturation and the slow injection of the 30% saturation solution look of similar size, whereas the fast injection of 30% saturated solution produced the largest crystals. Therefore the rate of solution injection as well as the degree of saturation may have an effect on the product characteristics. All of the experiments produced small needlelike particles, which is typical of methylprednisolone acetate from tetrahydrofuran. The residual THF was measured by capillary GC and was found to be very low in three of the four cases. The quality of each product was GT 99.1 wt. % by HPLC, which is as good as the starting material used.

Although all of the experiments further reported in this article were done with 85–95% saturated injection solution (unless otherwise noted), it seems as if backing away from nearly saturated solution may be a better choice for the preparation of the small uniform particles. Of course, this does not help the powder production rate or the processing costs.

The effect of different injection solvents

The choice of organic solvent used to dissolve the compound to be microprecipitated is primarily one of choosing a solvent with an adequate solubility for the solute and miscibility with the antisolvent. Most organic solvents are miscible with either carbon dioxide or ethane at least in the range 0–15 mol %, which is the usual maximum concentration of injection solvent that develops in the autoclave at steady state. The unfortunate exception is water. The solubility of water in carbon dioxide (0.33 mol % at 101 bar and 25°C) and in ethane (0.093 mol % at 36.0 bar and 25°C) is so low (Coan and King, 1971) that a second phase forms (probably) almost immediately in the mixing chamber when water is introduced. For now, water-soluble compounds such as organic or inorganic sodium or potassium salts must be dissolved in methanol or dimethylformamide or alternative carrier solvents in order to obtain good results. When water has been tried, even in such combinations as 15% H_2O/85% methanol, the results are low yield of a sintered powder due to the fact that a second phase of water apparently forms in the autoclave and redissolves the precipitated product (if any), thus allowing it to pass

Table 10. Saturation of Solute in Injection Solution on Particle Properties

Run % Sat.	Temp. °C	Pres. bar	Dens. g/cm^3	CO_2 Flow g/min	Inj. Flow mL/min	Inj. Conc.* g/mL	Yield wt. %	Tapped Sp. Vol. cm^3/g	Part. Size μm	Resid. THF wt. %
1 (60%)	16	154	0.927	66	2.60	0.066	99.0	12.9	2.7	0.05
2 (90%)	14	154	0.936	71	2.43	0.087	100.0	8.2	3.2	0.04
3 (30%)	14	152	0.935	70	2.53	0.056	94.5	13.1	5.4	0.05
4 (30%)	10	152	0.954	65	4.92	0.056	100.0+†	8.4	5.8	0.49

*Saturation for methylprednisolone acetate in THF at 20°C is 0.095 g/mL.
†This run yielded 101 wt. % recovery, as if too much material was inadvertently charged.

Table 11. Effect of Different Carrier Solvents with CO_2/MRA

Solvent	Temp. °C	Pres. bar	Dens. g/cm³	CO_2 Flow g/min	Inj. Rate mL/min	Yield wt. %	Resid. Solv. wt. % GC	Part. Size μm
THF	26	126	0.839	75.0	4.0	91.7	0.05	5.8
Dimethylacetamide	22	122	0.860	82.0	2.8	75.4	0.00	11.6
15% MeOH/85% CH_2Cl_2	24	125	0.851	90.0	3.2	77.6	0.01 MeOH 0.04 CH_2Cl_2	5.3
15% MeOH/85% CH_2Cl_2	24	123	0.848	68.0	2.8	68.0	0.00 MeOH 0.04 CH_2Cl_2	6.8
1,3-Dioxolane	24	125	0.851	57.0	4.1	32.8	LT 0.03	5.9
THF (Repeat)	25	121	0.840	82.0	4.2	66.0	0.03	6.5

through the collection filter plate. A few percent water (2% or less) added to tetrahydrofuran has worked well; the presence of water needed to attempt to alter the crystal form (or habit) of methylprednisolone acetate in one experiment.

Different choices of injection solvent primarily influence the size of the particle formed and the appearance of the particles by microscopic examination. For methylprednisolone acetate, THF always gives small rods with high aspect ratio. 1,3-Dioxolane, a cyclic ether similar to THF, also gave rods, but the yield was lower, probably due to the higher solubility of MRA in dioxolane than THF (Table 11). Methylene chloride (85%)/methanol (15%) mixed solvent generally gave the smallest particles, but the particles were broken shards as seen under the microscope; more spherical, although the crystal form was the same by XRD. Dimethylformamide, the least volatile but strongest solvent examined, produced the largest particles. Our rule for initially choosing the carrier solvent is to use the most volatile solvent possessing good solubilizing power for the solute. If unsatisfactory results are obtained, other carrier solvents are tried. The amount of residual solvent remaining in the product is a concern for powders of pharmaceutical application (Yeo et al., 1993). Listed in Table 11 are some values for the amount of residual solvent found in the products by capillary gas chromatography.

The effect of carbon dioxide vs. ethane as an antisolvent

As seen throughout Tables 2–11, ethane and carbon dioxide are essentially interchangeable, and other factors such as injection temperature can be used to control particle size and bulk-powder density. Based on our experience, for all other process variables being held the same, ethane tends to give slightly smaller particles and a more voluminous powder with the majority of the solutes that we have tried. In one case (the only case where it has been examined), special capillary GC revealed a small amount of ethane (0.05 wt. %) in the finished near-critically microprecipitated solid. The solid was a nonsteroid pharmaceutical. This presents the possibility that carbon dioxide may also be present in trace amounts, but cannot be seen reliably with gas chromatography.

Mathematical Modeling

The equations governing the microprecipitation can be derived by performing an unsteady-state mass balance around the autoclave precipitation chamber as shown in Figure 3. This derivation is essentially that of a simple CSTR with step change in inlet composition, but is complicated slightly by the two independent inlet flow rates and three components (Hill, 1977).

Let

$\dot{M}_A = CO_2$ inlet rate (const.) (g/min)
$\dot{F}$ = Solution feed rate (const.) (g/min)
$\dot{D}$ = Discharge rate (const.) (g/min)

Make assumptions:

1. System initially (flowing S.S.) pure "A."
2. At $t = 0$, F is turned on at constant rate.
3. Well mixed. Outlet composition = system composition.
4. The volume occupied by the solid is negligible.
5. The solid has negligible solubility in CO_2.

Further, the system is divided into two phases:

1. A fluid phase M_f^{sys} comprised only of $A + B$.
2. A solid phase $M_C^{sys} = S(t)$, which is pure C.

$$\frac{dM_{tot}^{sys}}{dt} = \text{Rate of } A, B, C \text{ in} - \text{rate of } A, B \text{ out.} \quad (5)$$

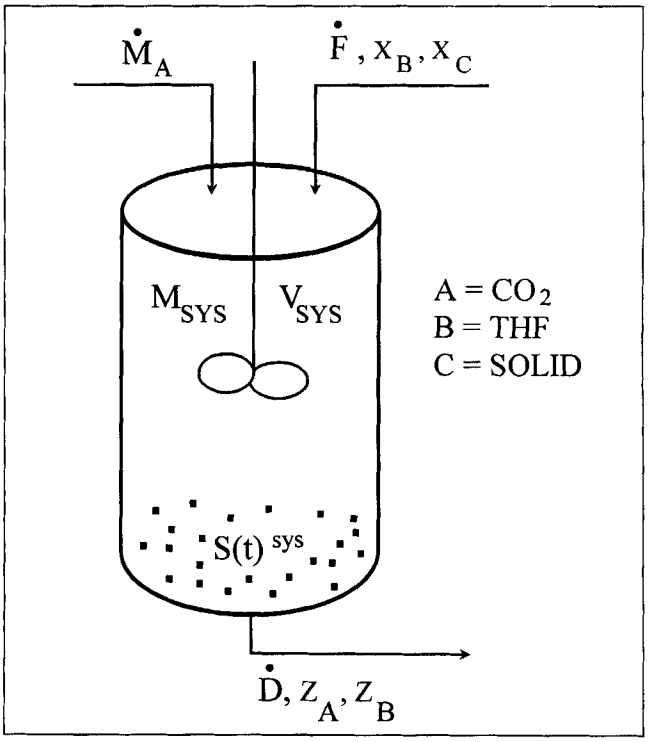

Figure 3. Microprecipitation chamber flow model.

For component A (CO_2),

$$\frac{dM_A^{sys}}{dt} = \dot{M}_{A,in} - \dot{M}_{A,out}, \tag{6}$$

but

$$M_A^{sys} = z_A M_f^{sys}, \tag{7}$$

so

$$\frac{dM_A^{sys}}{dt} = z_A\left(\frac{dM_0^{sys}}{dt}\right) + M_0^{sys}\left(\frac{dz_A}{dt}\right). \tag{8}$$

From Eq. 6

$$M_0^{sys}\left(\frac{dz_A}{dt}\right) = \dot{M}_{A,in} - \dot{M}_{A,out}, \tag{9}$$

but

$$\dot{M}_{A,out} = z_A \dot{D}. \tag{10}$$

Now approximate that the mass of the fluid phase remains constant with time (equal to M_0^{sys}), although composition changes. Then, outlet rate

$$\dot{D} = \dot{M} + x_B \dot{F}. \tag{11}$$

Let

$$\tau = \frac{\dot{M}_A}{M_0^{sys}} \equiv \text{min}^{-1}, \text{ an antisolvent time constant} \tag{12}$$

and

$$\chi = \frac{x_B \dot{F}}{M_0^{sys}} \equiv \text{min}^{-1}, \text{ a carrier solvent time constant.} \tag{13}$$

Combining Eqs. 9, 10, 11, 12, 13 and rearranging,

$$\frac{dz_A}{[\tau - (\tau + \chi) z_A]} = dt. \tag{14}$$

The boundary condition is at $t = 0$, $z_A = 1$ (pure CO_2). With this condition, one obtains

$$z_A = \frac{\tau}{\tau + \chi} + \frac{\chi}{\tau + \chi} e^{-(\tau+\chi)t}, \tag{15}$$

or

$$z_A = \left(\frac{\dot{M}_A}{\dot{M}_A + x_B \dot{F}}\right) + \left(\frac{x_B \dot{F}}{\dot{M}_A + x_B \dot{F}}\right)\left[\exp - \left(\frac{\dot{M}_A + x_B \dot{F}}{M_0^{sys}}\right) t\right] \tag{16}$$

and

$$z_B = 1 - z_A. \tag{17}$$

As $t \to \infty$, the equation asymptotes,

$$z_B^{\infty} = \frac{x_B \dot{F}}{\left(\dot{M}_A + x_B \dot{F}\right)}. \tag{18}$$

When the injection is complete, pure antisolvent is continued to be pumped through the mixing chamber to reduce the carrier solvent concentration to a low level. Beginning with an antisolvent composition z_A^0 at the end of the injection (t^0) and proceeding to an arbitrarily pure level z'_A, one arrives at the equation of the purge as

$$z'_A = (z_A^0 - 1)\left\{\exp - \left[\frac{\dot{M}_A}{M_0^{sys}}(t - t^0)\right]\right\} + 1. \tag{19}$$

Since the autoclave chamber initially holds about 1 kg of carbon dioxide, we purge with about 2.5 kg of pure antisolvent, and have found this satisfactory. A plot of how the carrier solvent concentration increases with time, and is then reduced by the purge, is shown in Figure 4 for three different injection rates approximately 2.48 mL/min (an actual experimental feed rate), 4.96, and 7.44 mL/min. The rate at which carbon dioxide is fed (66.0 g/min or $\tau = 4.260\ \text{min}^{-1}$) is constant in each simulation. When ethane is used at equivalent reduced temperature and pressure ($T_r = 0.964$ and $P_r = 2.03$), the concentration of carrier solvent attains higher levels in the mixing chamber because the initial mass of ethane in the chamber is less than with carbon dioxide. This mass balance model can be used for cost analysis optimization if dollar value amounts are tied to the streams.

Conclusions

Supercritical fluid microprecipitation is a novel technique that complements SCF rapid expansion powder formation techniques. Solutes that are sparingly soluble in supercritical fluids can now be formed with small particle size, high yield, low bulk-powder density, and moderately high specific surface area. Several processing variables influence the outcome of the microprecipitation. Lower temperatures (subcritical antisolvent) generally gives more voluminous powder, and injecting warm injection solution into cold antisolvent favors

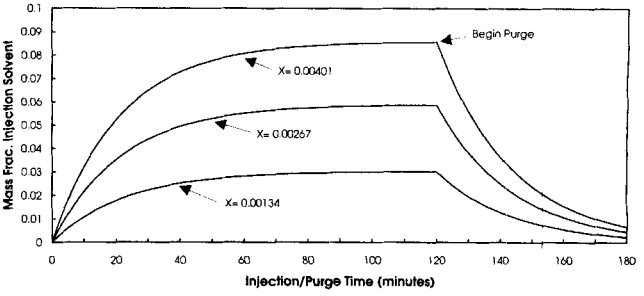

Figure 4. Fluid composition in precipitation chamber.

smaller particles. In some cases ethane gives a more desirable product and in other cases carbon dioxide is favorable. Comparisons of these trends with those reported elsewhere for polymeric solutes are generally in good agreement where applicable (Dixon et al., 1993).

Acknowledgments

The authors sincerely wish to acknowledge the contributions of many people in this work, including Sandra J. Howard and Alice E. DeJong for their excellent manuscript preparation. We also wish to acknowledge J. A. Campbell, C. E. Sacks, R. H. Meury, A. G. Padilla, V. A. Berglund, O. M. Smith, D. M. Gray, and D. P. Carvell for their contributions to this work.

Notation

D = discharge (filtrate) stream
F = injection (or carrier) solution
M = mass of component or phase
S = mass of solid solute
x, z = inlet and outlet mass fractions

Greek letters

τ = antisolvent time constant
χ = carrier solvent time constant

Superscripts and subscripts

A = antisolvent
B = carrier solvent
C = solute
0 = initial
f = fluid phase
r = reduced property
act = actual (amount)
sat = saturated
$'$ = purge cycle

Literature Cited

Angus, S., B. Armstrong, K. M. de Reuch, V. V. Altunin, O. G. Gadetskii, G. A. Chapela, and J. S. Rowlinson, *IUPAC International Thermodynamic Tables of the Fluid State Carbon Dioxide*, Pergamon Press, New York (1973).

Coan, C. R., and A. D. King, Jr., "Solubility of Water in Compressed Carbon Dioxide, Nitrous Oxide, and Ethane: Evidence for Hydration of Carbon Dioxide and Nitrous Oxide in the Gas Phase," *J. Amer. Chem. Soc.*, **93**, 1857 (1971).

Debenedetti, P. G., and J. W. Tom, "Particle Formation with Supercritical Fluids—A Review," *J. Aerosol Sci.*, **22**, 555 (1991).

Dixon, D. J., K. P. Johnston, and R. A. Bodmeier, "Polymeric Materials Formed by Precipitation with a Compressed Fluid Antisolvent," *AIChE J.*, **39**, 127 (1993).

Fischer, W., "Method and Apparatus for the Manufacture of a Product Having a Substance Embedded in a Carrier," U.S. patent 5,043,280 to Schwarz Pharma AG (Aug. 27, 1991).

Gallagher, P. M., M. P. Coffey, V. J. Krukonis, and N. Klasutis, "Gas Antisolvent Recrystallization: New Process to Recrystallize Compounds Insoluble in Supercritical Fluids," *Supercritical Fluid Science and Technology*, K. P. Johnston and J. M. L. Penninger, eds., Amer. Chem. Soc. Symp. Ser., No. 406, p. 334 (1989).

Gaven, J. V., W. H. Stockmayer, and J. S. Waugh, "Self-Diffusion and Impurity-Controlled Proton Relaxation in Liquid Ethane," *J. Chem. Phys.*, **37**, 1188 (1962).

Goodwin, R. D., H. M. Roder, and G. C. Straty, *Thermophysical Properties of Ethane, from 90 to 600 K at Pressures to 700 Bar*, National Bureau of Standards, Boulder, CO (Aug., 1976).

Hill, C. G., Jr., *An Introduction to Chemial Engineering Kinetics and Reactor Design*, Wiley, New York, p. 277 (1977).

Kirk-Othmer, *Encyclopedia of Chemical Technology*, M. Grayson, ed., 3rd ed., Vol. 7, Wiley, New York, p. 261 (1979).

Matson, D. W., K. A. Norton, and R. D. Smith, "Making Powders and Films from Supercritical Fluid Solutons," *Chemtech*, p. 480 (Aug., 1989).

McCabe, W. L., and J. C. Smith, *Unit Operations of Chemical Engineering*, 3rd ed., McGraw-Hill, New York, p. 859 (1976).

Norwood, K. W., and A. B. Metzner, "Flow Patterns and Mixing Rates in Agitated Vessels," *AIChE J.*, **6**, 432 (1960).

Paulaitis, M. E., V. J. Krukonis, R. T. Kurnik, and R. C. Reid, "Supercritical Fluid Extraction," *Rev. Chem. Eng.*, **1**, 2 (1983).

Reid, R. C., J. M. Prausnitz, and B. E. Polig, *The Properties of Gases and Liquids*, 4th ed., McGraw-Hill, New York, p. 637 (1987).

Schmitt, W. J., and R. C. Reid, "Solubility of Monofunctional Organic Solids in Chemically Diverse Supercritical Fluids," *J. Chem. Eng. Data*, **31**, 204 (1987).

Stahl, E., K. W. Quirin, A. Glatz, D. Gerard, and G. Rau, "New Developments in the Field of High-Pressure Extraction of Natural Products with Dense Gases," *Ber. Bunsenges. Phys. Chem.*, **88**, 900 (1984).

Yeo, S. D., G. B. Lim, P. G. Debenedetti, and H. Bernstein, "Formation of Mircoparticulate Protein Powders Using a Supercritical Fluid Antisolvent," *Biotech. Bioeng.*, **41**, 341 (1993).

Manuscript received Sept. 13, 1994, and revision received Jan. 27, 1995.